Journal of Alloys and Compounds 509 (2011) 2952–2956

Contents lists available at ScienceDirect

Journal of Alloys and Compounds

journal homepage: www.elsevier.com/locate/jallcom

Spatial stress distribution and optical properties of GaN films grown on convex shape-patterned sapphire substrate by metalorganic chemical vapor deposition

Tae Su Oh[a], Ah Hyun Park[b], Hyun Jeong[b], Hun Kim[b], Tae Hoon Seo[b], Yong Seok Lee[b], Mun Seok Jeong[c], Kang Jea Lee[b], Eun-Kyung Suh[a,b,*]

[a] Department of Nano Semiconductor & Display, Semiconductor Physics Research Center, Chonbuk National University, Jeonju 561-756, Republic of Korea
[b] School of Semiconductor & Chemical Engineering, Semiconductor Physics Research Center, Chonbuk National University, Jeonju 561-756, Republic of Korea
[c] Advanced Photonic Research Institute, Kwangju Institute of Science and Technology, Kwangju 500-712, Republic of Korea

ARTICLE INFO

Article history:
Received 3 October 2010
Received in revised form
15 November 2010
Accepted 19 November 2010
Available online 30 November 2010

PACS:
71.55.Eq
78.30 Fs
78.47jd
78.55Cr
81.15.Gh

Keywords:
GaN
Metalorganic chemical vapor deposition
Convex-shaped patterned sapphire
Micro-Raman scattering
Micro-photoluminescence

ABSTRACT

μ-Raman and μ-photoluminescence methods have been employed to investigate microscopic spatial stress distribution and optical properties of GaN films grown on the convex shape-patterned sapphire substrate (CSPSS). By comparison of the μ-Raman and μ-PL spectra, we found that significantly large difference, $\Delta\sigma_{xx}$ ~0.46 GPa, in biaxial compressive stress between the flat trench and convex regions in the side facet of the GaN film, around ~2 μm below the surface whereas on the GaN surface, little difference with large residual stress was observed in both regions compared to those from the side facet. Temperature dependent and time-resolved photoluminescence spectra have shown that the GaN film grown on the CSPSS has improved crystal purity through the reduction of intrinsic point defects.

1. Introduction

Gallium nitride (GaN) is one of the promising materials used in optoelectronic devices such as visible/ultra-violet light emitting diodes (LEDs) [1,2]. In the pursuit of the GaN growth with improved structural and optical properties, the use of the patterned sapphire substrate (PSS) technique has been shown to be effective in reducing the defect density in the GaN layer [3,4]. Further, it is well known that this method can efficiently extract the light trapped or/and wave-guided in GaN-based LED epistructures by total internal reflection. Although, there have been much research on the superior properties of the GaN films grown with a PSS method, most have focused mainly on the characteristics of the GaN films grown on conventional PSS which has an abrupt or inclined surface shape [3–5] because of the difficulty in fabricating a curved facet of sapphire which has been widely used as a substrate. Recently, InGaN/GaN-based LEDs fabrication and GaN epi-growth on the PSS with curved facets such as a microlens or hemispherical shape have been reported [6–8], but detailed optical studies on the GaN film grown on the PSS with a curved surface shape are only few until now. From the use of the PSS with a curved shape, we can expect that the properties of a GaN film are different in view of luminescence behavior and local stress distribution compared to that of the reference GaN film grown on a conventional patterned sapphire.

In this work, the GaN films have been grown on the convex shape-patterned sapphire substrate (CSPSS) by using metalorganic chemical vapor deposition (MOCVD). To study the microscopic spatial stress distribution and luminescence properties of the GaN films grown on CSPSS, micro-Raman (μ-Raman) spectroscopy and micro-photoluminescence (μ-PL) measurements were carried out, and macroscopic optical properties of the GaN films grown on conventional sapphire and CSPSS were characterized by temperature dependent photoluminescence (TDPL) and time-resolved photoluminescence (TRPL), respectively.

* Corresponding author at: Department of Nano Semiconductor & Display, Semiconductor Physics Research Center, Chonbuk National University, Jeonju 561-756, Republic of Korea. Tel.: +82 63 270 3606; fax: +82 63 270 3585.
E-mail address: eksuh@chonbuk.ac.kr (E.-K. Suh).

0925-8388/$ – see front matter © 2010 Elsevier B.V. All rights reserved.
doi:10.1016/j.jallcom.2010.11.166

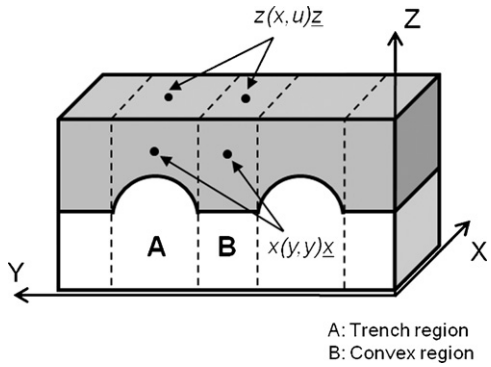

Fig. 1. Schematic view of the GaN film grown on a CSPSS and the corresponding μ-Raman configuration. Arrowed dots indicate the measured position, where the Raman spectra were recorded.

2. Experimental procedure

The GaN films were grown on a *c*-axis oriented CSPSS by MOCVD. For comparison, a reference GaN film was grown on flat sapphire substrate. The CSPSS was prepared by the thermal photo-resist (PR) reflow [9] and dry etching method. It revealed that the patterned sapphire had the appearance of a hemispherical shape array with a smoothly curved surface. Prior to the loading into the MOCVD reactor, the CSPSS was treated by a chemical cleaning process consisting of rinsing in deionized water for 5 min and isopropyl alcohol at 50 °C for 1 min, and drying by nitrogen. During the MOCVD growth, trimethylgallium (TMGa) and ammonia (NH_3) have been used as the precursor materials of Ga and N, respectively, and hydrogen as a carrier gas. The GaN film has been grown on CSPSS using a conventional two-step growth method with a low temperature (LT) GaN buffer layer; the LT buffer layer was grown at a temperature of 535 °C for 205 s and the growth of the GaN film was followed at 1050 °C for 90 min. The thickness of the GaN film was estimated to be ~3.5 μm. The μ-Raman scattering, which is sensitive to microscopic structural disorder and internal stress, was performed at room temperature. The GaN films were excited both parallel and perpendicular to the sample surface depending on the scattering geometry using a 632.8 nm He–Ne laser. The scattered light was detected in backscattering geometry which correspond to either $z(x,u)\underline{z}$, or $x(y,y)\underline{x}$ configurations. The schematic epistructure of the GaN on CSPSS and corresponding Raman scattering configuration is shown in Fig. 1. The *z*-direction in the scattering configuration was chosen along the *c*-axis of the GaN film. The dark dots indicate the positions where Raman spectra were recorded. The μ-Raman spectra were excited from two different positions on the top surface and on the side facet located ~2 μm below the GaN surface of the convex and flat trench regions, respectively, as marked with dots in Fig. 1. In μ-PL measurement, a continuous wave beam from a 355 nm of diode laser was used as an excitation source. The spatial resolution in the μ-PL was estimated to be sub-micron size. For the TDPL, GaN samples were placed in a closed cycle He cryostat with temperature range from 11 to 250 K and excited with the 325 nm line of a He–Cd laser. The TRPL measurements were carried out using a tunable femto-second (fs) pulsed laser system consisting of a second-harmonic generation of Ti:sapphire laser and a streak camera for detection. The pulse width and repetition rate were 100 fs and 76 MHz, respectively.

3. Results and discussion

Fig. 2 shows typical μ-Raman spectra of the GaN film grown on CSPSS and reference GaN film, recorded from both the top surface and side facet. There are three major peaks associated with the E_2 (high), A_1 (LO) and A_1 (TO) modes. All observed modes of the GaN are consistent with the selection rules in the $z(x,u)\underline{z}$ and $x(y,y)\underline{x}$ configurations. In μ-Raman spectra from the side facet of the GaN film under the $x(y,y)\underline{x}$ geometry, relatively intense E_2 (high) and A_1 (TO) peaks were observed from the trench region compared to those from the convex region and from the reference sample. The full width at half maximum (FWHM) value of the E_2 (high) peaks determined by a Lorentzian function fitting were estimated to be 3.5, 3.75 and 3.64 cm^{-1} for trench, convex regions and reference GaN, respectively implying an improvement in the crystalline quality in the trench region. Also, we observed a non-Gaussian A_1 (LO) peak near 735.3 cm^{-1}, which may be the result of unintentional n-type doping of the GaN film. In $x(y,y)\underline{x}$ configuration, the frequencies of the E_2 (high) mode, which was used for stress calibration, were found to be 569.9 (convex region), 568.9 (trench region), and 570.4 cm^{-1} (reference GaN). Compared with a standard frequency value 567.6 cm^{-1} of the unstrained bulk GaN film for an E_2 (high) mode [10], we found that a higher degree of stress relief was achieved in the GaN film on the trench region than that on the convex region of the CSPSS. In the case of the Raman spectra recorded from the surface under a $z(x,u)\underline{z}$ scattering configuration, the E_2 (high) modes recorded from a reference GaN film were shifted towards the lower frequency from 570.4 to 569.2 cm^{-1}, indicating compressive-strain relaxation during the typical MOCVD growth. In contrast, the E_2 (high) peaks from the surface of both the convex and flat trench regions appeared at higher frequencies than those of peaks obtained from the side facet, implying the presence of significant residual stress at the surface of the GaN film.

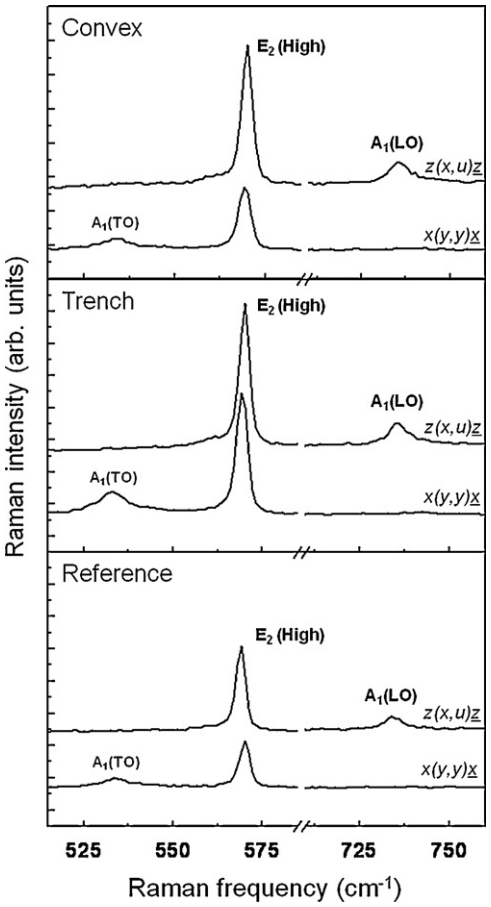

Fig. 2. μ-Raman spectra of the GaN film on CSPSS and reference recorded from the top surface and side facet of the convex and trench regions under different scattering geometry. The dashed line indicates a guide for the eyes for observing the peak position of the E_2 (high) phonon mode.

The frequency shift ($\Delta\omega$) in the E_2 (high) mode by the compressive strain can be expressed as $\Delta\omega$ (cm^{-1}) = $K\sigma_{xx}$ where K represents the linear stress coefficient (cm^{-1}/GPa). We determined the compressive stress (σ_{xx}) by adopting the theoretical value (2.56 cm^{-1}/GPa) for the stress coefficient given by Wagner and Bechstedt [11]. For the GaN film grown on a CSPSS, the variations of the biaxial compressive stress estimated from the frequency shift of E_2 (high) mode recorded from the top surface and from the side facet at 2 μm below the top surface are displayed as a function of position in Fig. 3. The scale of the scanning electron microscopy (SEM) image is identical to that marked on horizontal distance-axis. As mentioned earlier, higher degree of stress relief occurred inside GaN layer grown above the trench region; the average stress values at ~2 μm below the top surface of the GaN film were evalu-

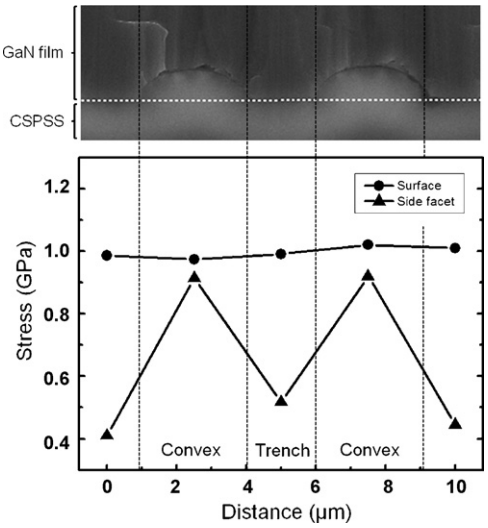

Fig. 3. Subsequent variation of biaxial compressive stress recorded at the top surface (filled circle) and side facet (filled triangle) of the GaN film grown on CSPSS. The scale of SEM image is identical to the scale of the *x*-axis.

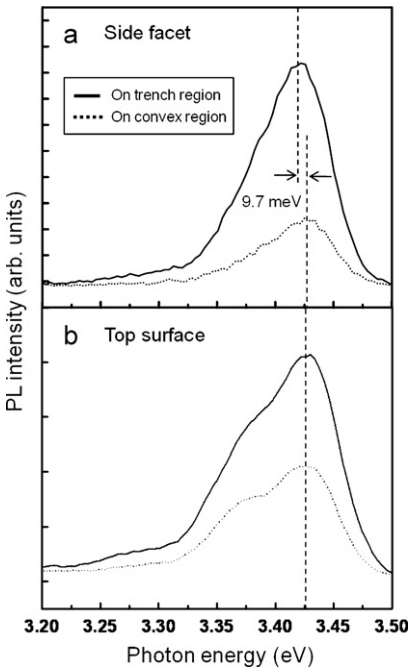

Fig. 4. μ-PL spectra of GaN films recorded at (a) the side facet of (b) the surface of the trench and convex regions.

ated to be 0.457 GPa above the trench region and 0.917 GPa above the convex region. A difference in compressive biaxial stress of $\Delta\sigma_{xx} \sim 0.46$ GPa observed between trench and convex regions. In our previous works [7], we observed strong cathodluminescence from trench regions and these results were attributed to the full coalescence by the lateral growth behavior on trench regions of CSPSS. Further, the results reported by Shin et al. have shown that the GaN buffer layer was not formed on convex shapes but only over the flat sapphire region, *i.e.,* flat trench region [12]. On the other hand, a high defect density has been persisted in the GaN grown on the convex region. Consequently, a large residual stress in the GaN film remained over the convex regions because of the large lattice mismatch between the GaN and sapphire substrate. Therefore, relatively small FWHM and stress relief from the GaN side facet at the convex regions can be directly associated not only with stress relaxation by lateral growth behaviors on the trench region but also to the absence of the GaN buffer layer. From the Raman spectra recorded in $z(x,-)\underline{z}$ geometry, the average biaxial stresses were estimated to be 0.979 and 0.984 GPa on the trench and convex regions, respectively. The stress degree at the surface of the GaN film grown on CSPSS was higher than that evaluated at 2 μm below the surface measured from the side facet of the GaN film. Further, there is little stress difference between both regions. Concerning the residual stress, this stress distribution differs from those reported previously, in which the relaxation of residual stress occurred as the coherent growth progresses [13,14]. This result is contributed to the thermal effect. Thermal compressive stress perpendicular to the *c*-axis is inevitably built in the film during a cooling step from GaN growth temperature due to large thermal mismatch. Such thermal stress causes large strain in the GaN film, especially near the GaN surface. In the case of a reference GaN, in contrast, the stress relief has appeared with coherent growth progresses as shown in μ-Raman spectra. It may result in compensation of thermal stress by relatively high dislocation density compared to that of the GaN film on CSPSS since dislocations have been known to relax stress.

Depending on the variation of internal residual stress, the microscopic luminescence properties of the GaN film were characterized by using μ-PL measurement. Fig. 4(a) denotes the room temperature μ-PL spectra measured from the side facet at the same point the Raman spectra were taken as shown in Fig. 1. The intensity of the near-band-edge (NBE) luminescence for the GaN grown on the trench region becomes stronger, by a factor of more than three, compared to that attained from the GaN grown above the convex region. It is well known that the NBE intensity is sensitive to defect density [15]. Hence, such a difference in the PL intensity between the trench and convex regions signifies a considerable decrease of the defect density. Furthermore, the PL spectra show local variations in the spectral peak position as well as in the luminescence intensity. The NBE luminescence from the trench region was red-shifted by 9.7 meV with respect to that obtained from the GaN film above the convex region. This value is in agreement with that expected from the biaxial compressive stress dependent shift, 23 meV/GPa, of the NBE luminescence peak position at room temperature [16], considering the difference in the stress degree at the points of interest on side facet of the trench and convex-shaped regions was measured to be 0.46 GPa, on average. Therefore, we can attribute this red-shift to the efficient relaxation of the residual compressive strain in the GaN grown at the trench region. Fig. 4(b) shows μ-PL spectra from the surface of the convex and trench regions of the GaN film. An increase in the NBE intensity was observed from the trench region. Also, the NBE peak positions are almost same, implying little difference of residual stress at the surface of trench and convex regions. This is in good agreement with surface stress distribution in μ-Raman results.

Macroscopic optical properties of the GaN film grown on the CSPSS were studied by photoluminescence (PL) spectra in the temperature ranged from 11 to 300 K, using a 325 nm line of a He–Cd laser. Fig. 5 illustrates typical PL spectra obtained from the GaN surface as a function of temperature. At low temperature, a neutral donor-bound exciton (D^0X), free excitons A and B (FX_A and FX_B) and a phonon replica (1-LO) are clearly distinguishable. These assignments have been confirmed by the evolution of the TDPL including the peak positions, quenching and the separations between the peaks. From the PL spectrum measured at 11 K, peak positions of the D^0X, FX_A and FX_B excitons for the GaN film grown on CSPSS were found to be 3.483, 3.489 and 3.498 eV, respectively. With increasing temperature, the PL spectra are dominated by the FX_A peak. Generally, misfit strain can generate extended defect structures such as threading dislocations (TDs), stacking faults and point defects, and

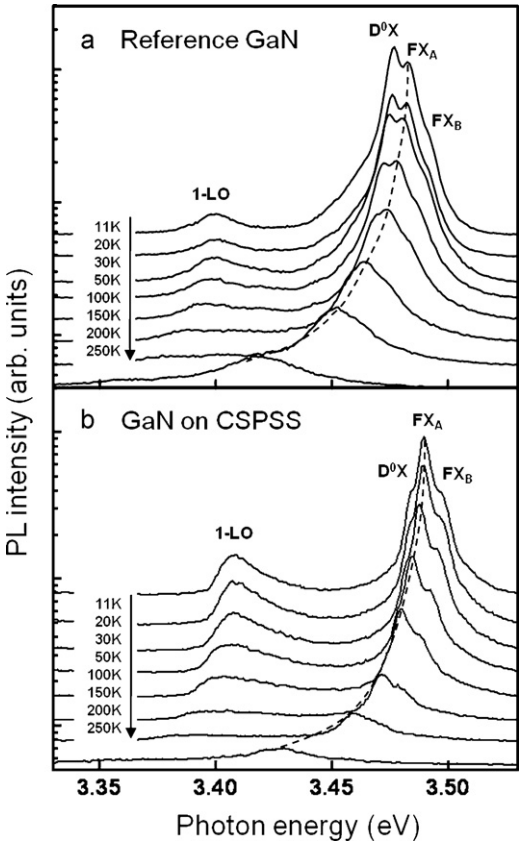

Fig. 5. TDPL spectra of (a) a reference GaN film and (b) the GaN film grown on a CSPSS. The dashed lines show the evolution of the FX_A peaks depending on temperature.

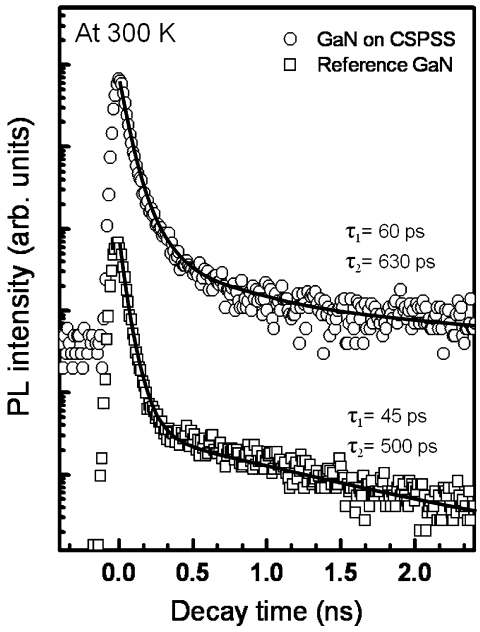

Fig. 6. Time-resolved decay profiles for centered PL emission of the GaN film grown on CSPSS and a reference GaN at room temperature, respectively.

thus, exert profound effects on the optical properties of the GaN film including the bandgap energy. In our case, the excitonic peaks at 11 K have been shifted by $\sim 6 \pm 2$ meV towards higher energies compared to the peak positions in the reference GaN film [Fig. 5(b)]. From the strong dependency of the bandgap energy on the strain present in a GaN film, these results correspond to a higher compressive stress at the surface of the GaN film grown on CSPSS as shown in Fig. 3. Compared to a reference GaN, other feature appearing in the TDPL spectra is the relatively intense FX_A peak of the GaN film with respect to the D^0X peak. In general, a bound exciton is known as an excited multiparticle state of a defect and especially, the D^0X exciton is believed to be related to an unidentified residual shallow donor associated with the presence of a vacancy as intrinsic point defects in the GaN film [17]. The dominant free exciton peaks may be evidence that the density of point defects in the GaN film grown on CSPSS is very low.

In order to further investigate this result, we carried out TRPL measurement. Fig. 6 shows the room temperature TRPL decay profiles of GaN films grown on a CSPSS and a reference GaN. The decay curves of the TRPL spectra are not of a single exponential form, but can be approximated by a superposition of two exponential decays with different relaxation time, τ_1 and τ_2. In general, the fast decay component τ_1 most probably represents the effective non-radiative recombination at room temperature while the slow decay component τ_2 is attributed to the radiative lifetime of the free exciton. The decay curves for GaN samples were fitted by a double-exponential decay function $[I(t) = A_1 \exp(-t/\tau_1) + A_2 \exp(-t/\tau_2)]$, and then the decay times, τ_1 and τ_1, were obtained by the optimized fitting. The measured decay times for the GaN films grown on the CSPSS were calculated to be $\tau_1 = 65$ and $\tau_2 = 630$ ps, respectively. It is notable that these decay times are longer than those from a reference GaN, *i.e.*, $\tau_1 = 45$ and $\tau_2 = 500$ ps. The relatively short decay time might be interpreted as evidence for a strong excitation transfer process to nonradiative recombination channels such as the dislocations, point defects and their complexes. Among these nonradiative defects, point defects which is main point defect with typical concentration of 10^{17} cm^{-3} have been considered to be limiting factors of PL emission efficiency rather than dislocations at room temperature because very short diffusion length of carriers in GaN prevents most of carriers from being captured into dislocations [18,19]. They can be mainly accumulated and linearly arranged around dislocations due to the stress field produced by edge-typed TDs [20]. Compared with a reference GaN film, thus longer decay times in GaN film grown on a CSPSS is attributed to the decrease of native point defects such as Ga and N vacancies. This might be responsible for the decrease of edge TDs, acting as traps for intrinsic point defects. The presence of the more dominant FX_A peak rather than the D^0X peak in the TDPL from the GaN film grown on a CSPSS, and the decrease of TDs at trench regions by lateral growth behavior and residual strain relief support well these TRPL results.

4. Summary

GaN films grown on a CSPSS were examined by μ-Raman spectroscopy and PL. We found that a difference in compressive biaxial stress of $\Delta\sigma_{xx} \sim 0.46$ GPa between the trench and convex-shaped regions in the side facet can be attributed to the absence of the GaN buffer layer at the curved facet of the convex regions as well as lateral growth behavior on trench region. On the surface, in contrast, the significant residual stress revealed in both regions. The effect of thermal expansion might lead to the large stress near GaN surface. Also, the results from TDPL and TRPL have shown that the GaN film on a CSPSS has improved crystal purity via the reduction of native point defects compared to that of a reference GaN.

Acknowledgements

This research was supported by the Ministry of Knowledge Economy (MKE) and Korea Industrial Technology Foundation

(KOTEF) through the Human Resource Training Project for Strategic Technology, and by Priority Research Centers Program through the National Research Foundation of Korea (NRF) funded by the Ministry of Education, Science and Technology (2009-0094032).

References

[1] E.F. Schubert, J.K. Kim, Science 308 (2005) 1274–1278.
[2] A. Khan, K. Balakrishnan, T. Katona, Nat. Photon. 2 (2008) 77–84.
[3] C.-C. Pan, C.-H. Hsieh, C.-W. Lin, J.-I. Chyi, J. Appl. Phys. 102 (2007) 084503.
[4] Y.P. Hsu, S.J. Chang, Y.K. Su, J.K. Sheu, C.T. Wen, L.W. Wu, C.H. Kuo, C.S. Chang, S.C. Shei, J. Cryst. Growth 261 (2004) 466–470.
[5] D.S. Wuu, W.K. Wang, W.C. Shih, R.H. Horng, C.E. Lee, W.Y. Lin, J.S. Fang, IEEE Photon. Technol. Lett. 17 (2005) 288–290.
[6] C.-T. Chang, S.-K. Hsiao, E.Y. Chang, Y.-L. Hsiao, J.-C. Huang, C.-Y. Lu, H.-C. Chang, K.-W. Cheng, C.-T. Lee, IEEE Photon. Technol. Lett. 21 (2009) 1366–1368.
[7] T.S. Oh, Y.S. Lee, H. Jeong, J.D. Kim, T.H. Seo, E.-K. Suh, Jpn. J. Appl. Phys. 47 (2008) 5333–5336.
[8] D.-H. Kang, E.-S. Jang, H. Song, D.-W. Kim, J.-S. Kim, I.-H. Lee, S. Kannappan, C.-R. Lee, J. Korean Phys. Soc. 52 (2008) 1895–1899.
[9] S.-H. Park, H. Jeon, Y.-J. Sung, G.-Y. Yeom, Appl. Opt. 40 (2001) 3698–3702.
[10] V.Y. Davidov, Y.E. Kitaev, I.N. Goncharuk, A.N. Smirnov, J. Graul, O. Semchinova, D. Uffmann, M.B. Smirnov, A.P. Mirgorodsky, R.A. Evarestov, Phys. Rev. B 58 (1998) 12899.
[11] J.-M. Wagner, F. Bechstedt, Appl. Phys. Lett. 77 (2000) 346–348.
[12] H.-Y. Shin, S.K. Kwon, Y.I. Chang, M.J. Cho, K.H. Park, J. Cryst. Growth 311 (2009) 4167–4170.
[13] F. Bertram, T. Riemann, J. Christen, A. Kaschner, A. Hoffmann, C. Thomsen, K. Hiramatsu, E. Shibata, N. Sawaki, Appl. Phys. Lett. 74 (1999) 359–361.
[14] Q. Liu, A. Hoffmann, A. Kaschner, C. Thomsen, J. Christen, P. Veit, R. Clos, Jpn. J. Appl. Phys. 39 (2000) L958–L960.
[15] L. Macht, J.L. Weyher, A. Grzegorczyk, P.K. Larsen, Phys. Rev. B 71 (2005) 073309.
[16] W.G. Perry, T. Zheleva, M.D. Bremser, R.F. Davis, W. Shan, J.J. Song, J. Electron. Mater. 26 (1997) 224–231.
[17] U. Kaufmann, M. Kunzer, H. Obloh, M. Maier, C.H. Manz, A. Ramakrishnan, B. Santic, Phys. Rev. B 59 (1999) 5561–5567.
[18] S.F. Chichibu, H. Marchand, M.S. Minsky, S. Keller, P.T. Fini, J.P. Ibbetson, S.B. Fleischer, J.S. Speck, J.E. Bowers, E. Hu, U.K. Mishra, S.P. DenBaars, T. Deguchi, T. Sota, S. Nakamura, Appl. Phys. Lett. 74 (1999) 1460–1463.
[19] A. Pinos, S. Marchnkevičius, M. Usman, A. Hallén, Appl. Phys. Lett. 95 (2009) 112108.
[20] J. Elsner, R. Jones, M.I. Heggie, P.K. Sitch, M. Haugk, Th. Frauenheim, S. Oberg, P.R. Briddon, Phys. Rev. B 58 (1998) 12571–12574.